PLOS ONE

RESEARCH ARTICLE

Mechanism and Reaction Pathways for Microcystin-LR Degradation through UV/H_2O_2 Treatment

Yafeng Liu, Jing Ren, Xiangrong Wang, Zhengqiu Fan*

Department of environmental science & engineering, Fudan University, Shanghai, 200433, China

* zhqfan@fudan.edu.cn

Abstract

Microcystin-LR (MCLR) is the most common cyanotoxin in contaminated aquatic systems. MCLR inhibits protein phosphatases 1 and 2A, leading to liver damage and tumor formation. MCLR is relatively stable owing to its cyclic structures. The combined UV/H_2O_2 technology can degrade MCLR efficiently. The second-order rate constant of the reaction between MCLR and hydroxyl radical (·OH) is $2.79(\pm0.23)\times10^{10}$ M^{-1} s^{-1} based on the competition kinetics model using nitrobenzene as reference compound. The probable degradation pathway was analyzed through liquid chromatography mass spectrometry. Results suggested that the major destruction pathways of MCLR were initiated by ·OH attack on the benzene ring and diene of the Adda side chain. The corresponding aldehyde or ketone peptide residues were formed through further oxidation. Another minor destruction pathway involved ·OH attack on the methoxy group of the Adda side chain, followed by complete removal of the methoxy group. The combined UV/H_2O_2 system is a promising technology for MCLR removal in contaminated aquatic systems.

CrossMark
click for updates

OPEN ACCESS

Citation: Liu Y, Ren J, Wang X, Fan Z (2016) Mechanism and Reaction Pathways for Microcystin-LR Degradation through UV/H_2O_2 Treatment. PLoS ONE 11(6): e0156236. doi:10.1371/journal.pone.0156236

Editor: Franck Chauvat, CEA-Saclay, FRANCE

Received: February 16, 2016

Accepted: May 11, 2016

Published: June 9, 2016

Copyright: © 2016 Liu et al. This is an open access article distributed under the terms of the Creative Commons Attribution License, which permits unrestricted use, distribution, and reproduction in any medium, provided the original author and source are credited.

Data Availability Statement: All relevant data within the paper and the Supporting Information files.

Funding: The authors have no support or funding to report.

Competing Interests: The authors have declared that no competing interests exist.

Introduction

Cyanotoxins are drinking water contaminants released by harmful strains of cyanobacteria, such as *Microcystis*, *Anabaena*, *Nostoc*, and *Oscillatoria* [1]. Microcystins (MCs), which contain a large family of cyclic heptapeptides, are one of the most toxic cyanotoxin species. The general structure of MCs is cyclo [-D-Ala-L-X-D-MeAsp-L-Z-Adda-D-Glu-Mdha-], in which X and Z are variable L amino acids. Over 90 MC variants have been identified, and microcystin-LR (MCLR) is the most common species found in contaminated aquatic systems [2]. Studies have shown that MCs inhibit protein phosphatases 1 and 2A, leading to liver damage and tumor formation [3]. In addition, sublethal doses of MCs in drinking water are considered one of the key factors in the unusually high occurrence of primary liver cancer [4, 5].

Owing to their cyclic structures, MCs are relatively stable under a wide range of pH values and temperatures. Many of the bodies of water worldwide from which drinking water is obtained exhibit cyanobacterial blooms, and consumption of cyanobacteria-contaminated drinking water is the main cause of exposure to MCs.

A variety of conventional water treatment technologies, including coagulation/sedimentation [6], activated carbon adsorption [7], and membrane separation [8], have been employed to remove cyanotoxins; however, these techniques are ineffective owing to the stable structure of cyanotoxins, so they can't eliminate or reduce the toxicity as the cyan toxins can't be removed from the environment thoroughly. Advanced oxidation processes (AOPs) have recently become an effective alternative for remediation or removal of MCs. AOPs typically involve production of hydroxyl radicals (·OH) as oxidizing species, which degrade target organic materials [9]. The rate constants are typically in the order of 10^8–10^{10} L mol^{-1} s^{-1}. Studies have shown that MCs in aqueous solutions are efficiently degraded by TiO_2/UV [10–12], Fenton and photo-Fenton [13, 14], and ultrasonic irradiation [15, 16] and that ·OH is mainly responsible for MC degradation. The reaction mechanisms and pathways involved in TiO_2/UV and ultrasonic irradiation have already been proposed [16–18]. Moreover, toxicity experiments demonstrated that degradation of intermediates and byproducts significantly eliminates toxicity of cyanotoxins [10, 12].

Combined UV/H_2O_2 technology efficiently degrades MCs [19, 20]. ·OH and UV direct photolysis are both primarily responsible for MCLR degradation in combined UV/hydrogen peroxide (H_2O_2) process. However, the reaction mechanism and reaction pathway of MCLR degradation in the UV/H_2O_2 process has never been well understood. Previous studies on UV/H_2O_2 treatment have shown that direct photolysis of target compounds is assumed to be negligible [21, 22]. However, earlier studies have shown [19] that MCLR degradation is obviously affected by direct photolysis and thus should be taken into consideration [23]. This paper aimed to determine the second-order rate constant of the reaction between MCLR and ·OH and to investigate the reaction pathways involved in the UV/H_2O_2 process.

Materials and Methods

Chemicals

This study adopted the chemicals used by Changlong Wu [23]. Standard MCLR was purchased from Sigma-Aldrich Co., Ltd. and HPLC-grade acetonitrile (ACN) was purchased from Tedia Co., (USA). H_2O_2 (30%, w/w), sodium sulfite, sodium hydroxide, and sulfuric acid were purchased from Shanghai Chemical Reagent Co., Ltd. (Shanghai, China). All reagents are of analytical grade. Ultrapure water was obtained using Milli-Q Water System (Millipore, Bedford, MA, USA).

Photochemical experiments

Photochemical experiments were performed according to the method described by Changlong Wu [23]. Commercial low-pressure Hg UV lamp (6 W, 254 nm) was used for illumination [S1]. The UV light intensity irradiating the surface of the sample solution was controlled by adjusting the distance between the UV lamp and the quartz bottle and was measured using a luxometer. All experiments were conducted at 25 ± 1°C under atmospheric pressure and UV intensity of 134 μW/cm^2 at 10 cm. The reaction began by introducing a predetermined dosage of H_2O_2 into 3 mL of sample solution in a quartz bottle and by turning on the UV lamp. The exposure time is 10 minutes. The pH of the solution was 5.8 in all experiments. We used 3 mL of 100 mg/L MCLR solution to identify the reaction intermediates.

Analysis

The method used in the analysis was previously described by Weihua Song [16]. MCLR was analyzed using an HPLC (Agilent 1200) with photodiode array detection under the following

conditions: the column used was ZORBAX SB-C18 column (5 μm, 4.6 mm×250 mm, Agilent, USA) and the mobile phase consisted of 40% ACN and 60% water, both containing 0.05% trifluoroacetic acid (TFA). The liquid chromatography-mass spectrometry (LC-MS) system used in this study consisted of a Dionex Ultimate 3000 HPLC Pump, a Dionex Ultimate 3000 autosampler, and a Bruker micrOTOF II Mass Spectrometer with an electrospray ionization source. The HPLC column used was ZORBAX SB-C18 column (5 μm, 4.6 mm×250 mm, Agilent, USA). Moreover, the injection volume of the treated sample was 80 μL, and the mobile phase used was water and ACN, both containing 0.05% TFA. Gradient elution was performed based on the method described by Liu *et al.* [18]. Mass spectral data were also obtained in the positive ion mode by full scanning from m/z 400 to 1200.

Rate Constant Calculation

Competition kinetics experiments were conducted to evaluate the rate constant (k_{OH}) between ·OH and MCLR. Nitrobenzene (NB) [$k_{OH} = 4.0\times10^9$ M^{-1} s^{-1}] was chosen as reference compound because NB is difficult to directly photodegrade and is easily analyzed by HPLC. Moreover, NB has been successfully applied in similar experiments [23, 24]. Direct photolysis can be expressed by Eq 1 [25].

$$-\frac{d[MCLR]}{dt} = k_d[MCLR] = k_{S,\ MCLR}\Phi_{MCLR}[MCLR] \quad (1)$$

where k_d is the pseudo-first-order reaction rate constant; $k_{S,\ MCLR}$ is the rate constant of first order reaction by MCLR (E $mol^{-1}s^{-1}$); and Φ_{MCLR} is the quantum of MCLR (percentage of excited stage photons).

Assuming that direct photolysis of NB is negligible, destruction rates of MCLR and NB can be expressed by Eqs 2 and 3, respectively.

$$r_{MCLR} = k_{OH,\ MCLR}[\cdot OH]_{SS} + k_{S,\ MCLR}\Phi_{MCLR}f_{MCLR} \quad (2)$$

$$r_{NB} = k_{OH,\ NB}[\cdot OH]_{SS} \quad (3)$$

where [·OH] SS is the steady-state concentration of ·OH. The fraction of UV absorbed by MCLR (f_{MCLR}) is determined by Eq 4.

$$f_{MCLR} = \frac{\varepsilon_{MCLR}[MCLR]}{\varepsilon_{H_2O_2}[H_2O_2] + \varepsilon_{NB}[NB] + \varepsilon_{MCLR}[MCLR]} \quad (4)$$

k_{OH} of MCLR can be calculated by Eq 5.

$$k_{OH,\ MCLR} = k_{OH,\ NB}\frac{r_{MCLR} - k_d f_{MCLR}}{r_{NB}} \quad (5)$$

Results and Discussion

·OH rate constant

In order to calculate the·OH rate constant, we use Nitrobenzene(NB) concentrations from 10 μM to 100 μM were added into MCLR working solution (5 μM), and the solutions were treated with UV/H_2O_2 process by using 500 μM of H_2O_2. To determine the reaction rate constant of direct photolysis, we treated 5 μM of NB-free MCLR working solutions with UV irradiation alone under the same conditions as that in UV/H_2O_2 treatment, including the same UV intensity, pH value, and temperature (Table 1). k_{OH} of MCLR was constant under various concentrations, and the average value was 2.79 (±0.23)×10^{10} M^{-1} s^{-1}.

Table 1. Parameters determined under different nitrobenzene concentrations.

$C_{NB}(\mu M)$	$C_{MCLR}(\mu M)$	r_{NB} ($M^{-1}s^{-1}$)	r_{MCLR} ($M^{-1}s^{-1}$)	f_{MCLR}	k_d ($M^{-1}s^{-1}$)	$k_{OH,MCLR}$ ($M^{-1}s^{-1}$)(×10^{10})
10.0	5.0	0.0638	0.4572	0.310	0.0362 (R^2 = 0.9124)	2.80
19.5	4.4	0.0525	0.3318	0.176	0.0375 (R^2 = 0.8925)	2.48
50.0	5.0	0.0544	0.3521	0.088	0.0362 (R^2 = 0.9124)	2.57
88.5	3.7	0.0292	0.2216	0.039	0.0401 (R^2 = 0.8792)	3.01
87.1	4.9	0.0416	0.3171	0.052	0.0368 (R^2 = 0.9237)	3.03
100.0	5.0	0.0292	0.2105	0.046	0.0362 (R^2 = 0.9124)	2.86

doi:10.1371/journal.pone.0156236.t001

In a detailed assessment of the reactivity of ozone and ·OH toward different cyanotoxins, a bimolecular rate constant of 1.0×10^{10} $M^{-1}s^{-1}$ was previously determined by the reaction of ·OH with MCLR [26]. Competitive kinetics with pulsed radiolysis and transient absorption measurements were employed to determine the reaction rate of ·OH with MCLR, and the reaction rate is 2.3 (±0.1)×10^{10} $M^{-1}s^{-1}$ [27]. The difference between these measured rate constants is possibly caused by variations in experimental conditions and in the methods of determination [27]. Moreover, the pH of the solution influences conformation, charge, or both and can exert pronounced effect on the reactivity of MCLR. The rate constant of 1.0×10^{10} $M^{-1}s^{-1}$ was also determined under phosphate-buffered conditions at pH 7 [26], whereas the rate constants were determined under natural pH both in this paper and in Song's study [27]. Hence, the results determined in this paper are closer to that reported by Song *et al.* [27] compared with that reported by Onstad *et al.* [26].

LC-MS identification of byproducts of MCLR subjected under combined UV/H_2O_2 treatment

To separate and detect the degradation products, considerably higher concentration of MCLR agent was employed for the degradation experiment compared with that found in the environment. The intermediates were characterized based on the MS peak area criteria: the peaks must have a signal-to-noise ratio of 3, and the peak areas of treated sample must be at least two times larger than that if the initial sample, if the peak was found in the initial sample [17]. The LC-MS analysis under various reaction times revealed 9 decomposition products at detectable levels (Table 2). Moreover, the structural assignments of the degradation products of MCLR

Table 2. Reaction intermediates of MCLR degraded by the combined UV/H_2O_2 treatment.

No.	*Peak (m / z)*	RT (min)
1	795.4	6.0
2	795.4	6.7
3	835.4	7.1
4	811.4	6.1
5	1029.5	10 ~ 18
6	1011.5	15 ~ 20
7	1045.5	18.2
8	1045.5	20.9
9	1027.5	21.2
10	1009.6	21.4
11	995.5	21.7
12	995.5	22.3
13	965.6	25.2

doi:10.1371/journal.pone.0156236.t002

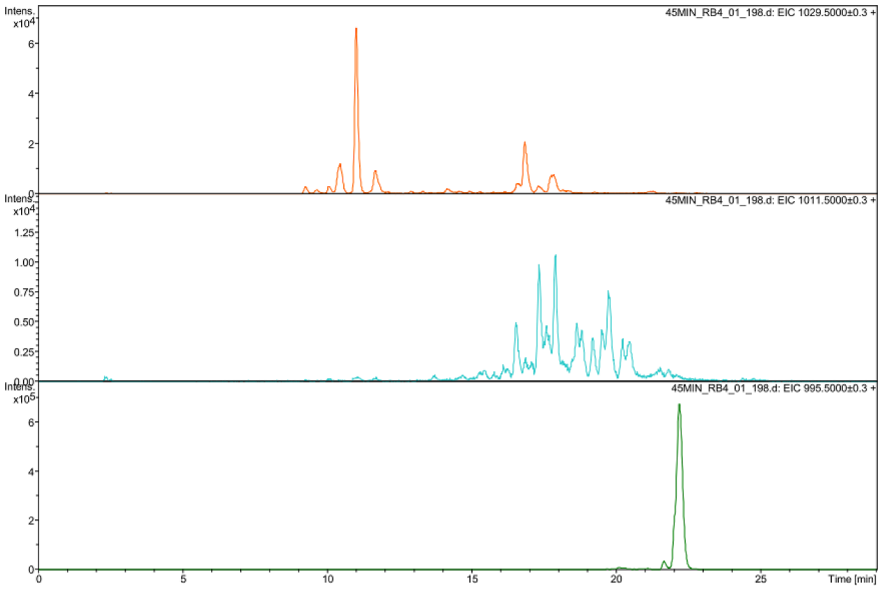

Fig 1. LC-MS chromatograph of MCLR after 45 min of UV/H_2O_2 treatment.

doi:10.1371/journal.pone.0156236.g001

from the combined UV/H_2O_2 treatment were based on the analysis of the total ion chromatogram (TIC) and on the corresponding mass spectra. The masses of the different products were determined from the $(M+H)^+$m/z peaks corresponding to the molecular ion [16].

The typical reaction between ·OH and target organic substance involves three competition pathways: addition, hydrogen abstraction, and electron abstraction. The rates of reaction of ·OH with different reaction sites in MCLR molecular vary significantly.

The product with $(M+H)^+$ at m/z 1029.5 was a major product and displayed a large time span in TIC (10 min < t < 18 min). This product corresponds to the addition of 34 mass units into MCLR and can result from addition of two ·OH into the diene in the Adda side chain through hydroxyl addition reaction. The first ·OH was incorporated into the double bond to form allyl radical (RCH = CH-R_2C·) and then a second ·OH reacted with the allyl carbon center to form the double hydroxylation derivative MCLR. The product ion $(M+H)^+$ at m/z 1029.5 during TiO_2 photocatalytic oxidation (PCO) was reported and assigned as a diol [12,18].

More than six peaks with a mass spectrum showing a molecular ion $(M+H)^+$ at m/z 1029.5 were observed in the TIC analysis (Fig 1). These products are proposed to be formed by geometrical isomerization of MCLR following UV_{254} irradiation and ·OH attack on the diene, leading to isomeric diols [18]. Under UV_{254} irradiation, the (4E), (6E) of the Adda configuration can be converted into (4E), (6Z) or (4Z), (6E) [28, 29], and this phenomenon was supported by the occurrence of two peaks corresponding to $(M+H)^+$ at m/z 995.5 in TIC (Table 2). Geometrical isomerization of MCLR provided precursors for the dihydroxyl-MCLR. In addition, double hydroxylation can occur on any of the double-bond pairs (C4-C5 and C6-C7) and can result in stereoisomeric forms of 1, 2- and 1, 4- dihydroxylated adducts of MCLR [17,27].

Dihydroxy-MCLR was further oxidized with cleavage of the dihydroxylated bond, resulting in different cleavage products depending on the location of the dihydroxy substitutes in the precursors. The $(M+H)^+$ ion at m/z 795.4 in the UV/H_2O_2 process is probably a cleavage products at positions C4-C5 on the Adda side chain, and the $(M+H)^+$ ion at m/z 835.4 is the cleavage products at positions C6-C7 on the Adda side chain. Moreover, the $(M+H)^+$ ion at m/z 811.3 is consistent with a carboxylic acid structure formed by bond cleavage of $(M+H)^+$ ion at m/z 795.4.

The $(M+H)^+$ ion at m/z 1011.5 intermediate was reported in other AOTs, such as ultrasonic irradiation [16] and PCOs. This ion corresponded to the addition of 16 mass units to MCLR and can result from addition of one ·OH into the diene or the aromatic ring in the Adda side chain through hydroxyl substitution reaction.

In the case of diene substitution reaction, an OH group substituted the hydrogen of C7 in the Adda side chain and formed an enol MCLR. The enol MCLR rapidly isomerized into a more stable tautomer of ketone MCLR, which then underwent a series of oxidation-induced bond cleavage reactions to form a ketone-derived ($(M+H)^+$ ion at m/z 835.4) and aldehyde-derived ($(M+H)^+$ ion at m/z 795.4).

In the case of aromatic substitution, the aromatic ring in the Adda side chain was attacked by ·OH, and the probable reaction mechanism involved the addition of one ·OH into one of the aromatic double bonds, forming a carbon-centered radical; the reaction of the carbon-centered radical with oxygen formed a peroxy radical, and finally, the elimination of hydroperoxyl radical yielded a phenolic derivative. In this case, *ortho*, *para*, or *meta* substitution usually occurs [16, 27]. The first aromatic hydroxylation increases the electron density of the aromatic ring and thus eletrophilic reactions (such as ·OH attack) proceed faster [16, 17, 30]. Therefore, the first hydroxylation of the aromatic ring was followed by a second one as demonstrated by detection of $(M+H)^+$ ion at m/z 1027.5, consistent with the result of addition of a second hydroxyl group to the phenyl group.

The reaction rates of the ·OH with different reaction sites present in MCLR are expected to vary significantly. The reaction rate of ·OH addition to the aromatic ring is the fastest among the competing processes because this process generally occurs at a nearly diffusion-controlled rate [16, 31]. This finding is also supported by the present study given that the m/z 1011.5 ion occurred at 2 min, whereas the other product ions did not occur until 5 min. Oxidation of both the conjugated diene and phenyl ring resulted in a product with $(M+H)^+$ ion at m/z 1045.5. This product was not observed in previous PCOs [18] but was observed in ultrasonic treatment [16, 32]. This product can undergo further oxidation of diol or cleavage of the diene, yielding a cleavage product (the $(M+H)^+$ ion at m/z 835.4) [16].

In addition, the reaction pathway involving the removal of methoxy group of the Adda chain has been observed in the analogous products during the UV/H_2O_2 process; this pathway was also proposed during PCO of MCLR [17]. The $(M+H)^+$ ion at m/z 1009.5 ion was assigned to the formic acid ester MCLR derivative, which was followed by complete removal of the methoxy group of Adda chain, thereby forming the $(M+H)^+$ ion at m/z 965.5 ion, DmADDA. These molecular ions are rarely observed in other AOT processes.

A summary of the proposed reaction pathways involved in the UV/H_2O_2 process are illustrated in Figs 2–4.

The relative concentration of the reaction products of MCLR was monitored using LC-MS as a function of treatment time (Fig 5). Given that the products exhibit similar structures, their response factors (peak intensity/molecule) were assumed to be similar, and their peak intensities were taken as indicator of their relative yields. The early appearance of the peaks was mainly assigned to the phenolic and diol products, and the reaction pathways involved accounted for over 90% of the total reactions.

Toxicity analysis of the degradation intermediates

Degradation of MCLR through the combined UV/H_2O_2 treatment was primarily caused by ·OH attack and direct photolysis. The main intermediates of MCLR decomposition through the combined UV/H_2O_2 process can be classified into two structural groups: group 1, consisting of ring peptides containing an Adda moiety ($(M+H)^+$ ion at m/z 1029.5, 1011.5, 1045.5,

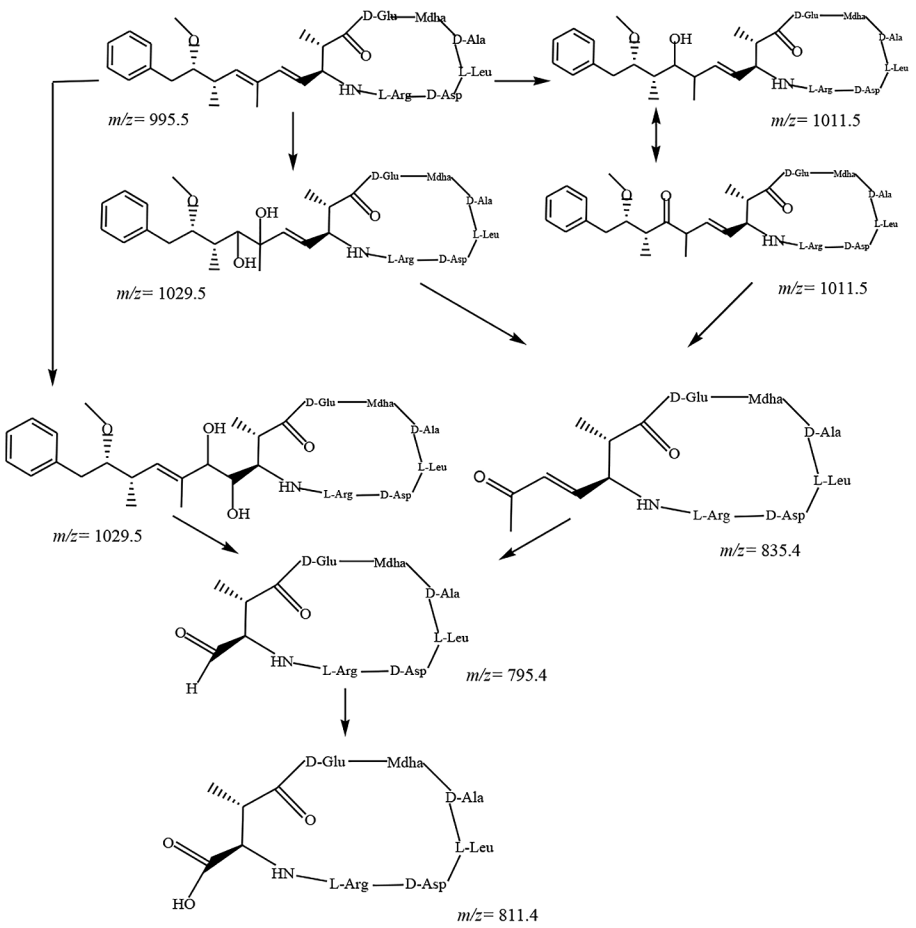

Fig 2. Byproducts and proposed reaction pathways for the combined UV/H_2O_2 degradation of the conjugated carbon double bonds of Adda side chain of MCLR.

doi:10.1371/journal.pone.0156236.g002

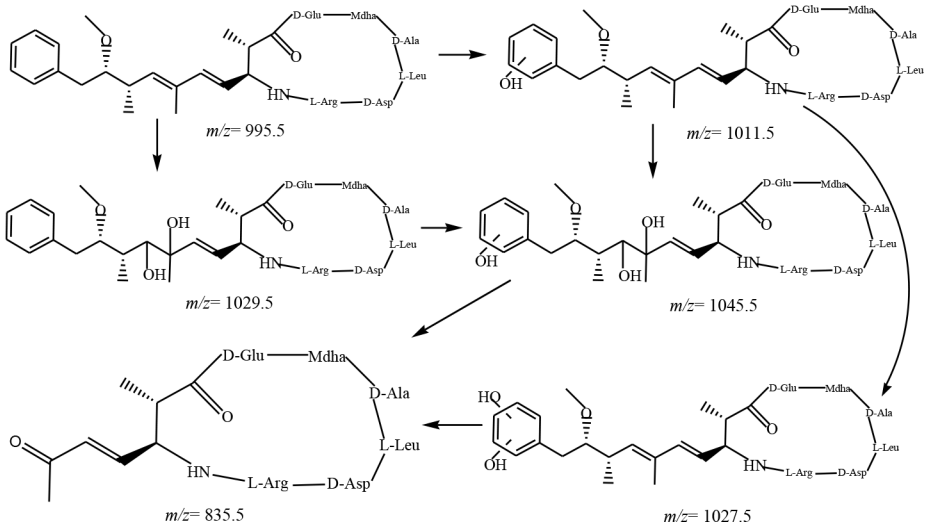

Fig 3. Byproducts and proposed reaction pathways for the combined UV/H2O2 degradation of the aromatic ring of Adda of MCLR.

doi:10.1371/journal.pone.0156236.g003

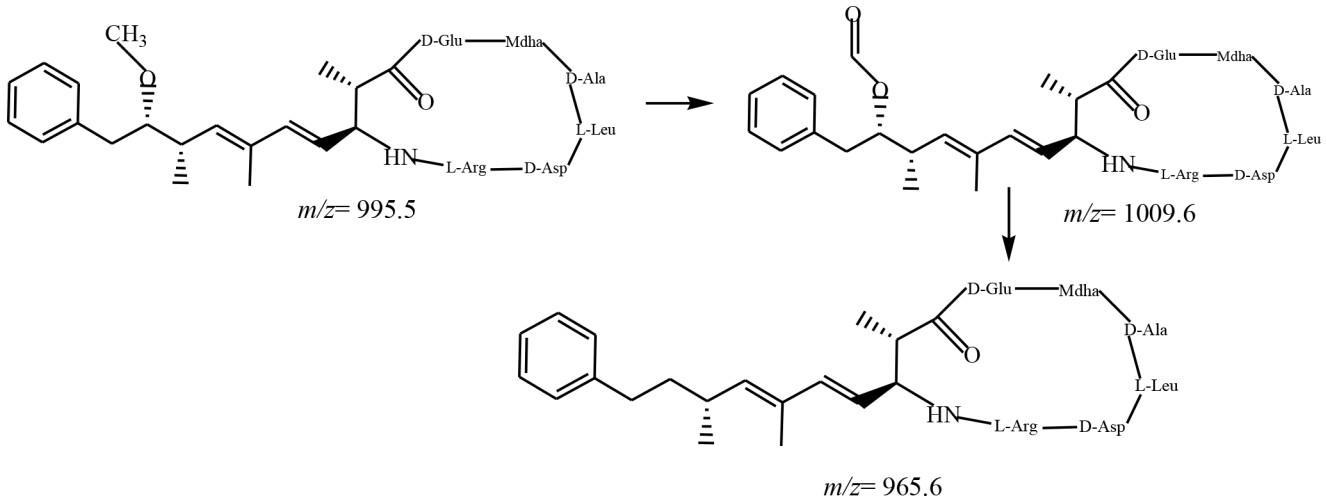

Fig 4. Byproducts and proposed reaction pathways for the combined UV/H2O2 degradation of the methoxy group of Adda of MCLR.

doi:10.1371/journal.pone.0156236.g004

1027.5, 1009.5, and 965.5); and group 2, consisting of ring peptides without an Adda moiety ($(M+H)^+$ ion at m/z 835.4, 795.4, and 811.3). Given that the conjugated diene structure of Adda in MCLR is essential for inhibition of protein phosphatases 1 and 2A [33, 34], the products of peptide residues without an Adda moiety are expected to be detoxified. Moreover, the other products, which underwent modification (e.g., dihydroxylation) in Adda side chain, also eliminate toxicity [33–35]. Therefore, the combination of UV/H_2O_2 is a promising technology for MC removal in bodies of water contaminated with cyanobacteria.

Conclusions

The combined UV/H_2O_2 system can effectively degrade MCLR in aqueous solution. Using nitrobenzene (NB) as competition reference compound, we developed a competition kinetic

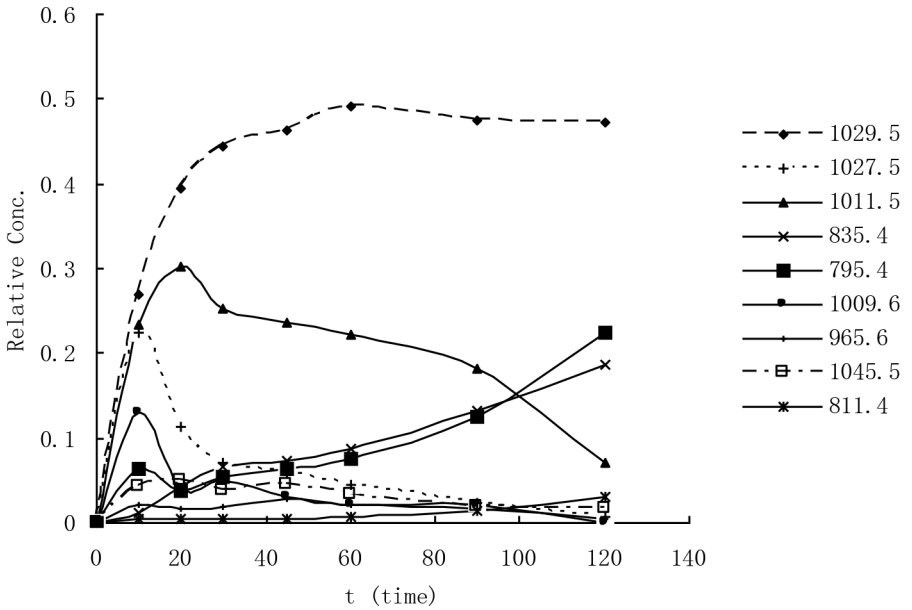

Fig 5. Relative yield of product ions versus time in the UV/H2O2 treatment.

doi:10.1371/journal.pone.0156236.g005

model for degradation of MCLR by UV/H_2O_2 by employing the pseudo-first-order equation and steady-state approximation. Using the competition kinetic model, we determined the second-order rate constant of the reaction between MCLR and ·OH to be 2.8 (±0.21)×10^{10} (M^{-1} s^{-1}).

MCLR degradation through UV/H_2O_2 treatment mainly involved ·OH attack, oxidation, and UV_{254} direct photolysis. The main sites of MCLR molecule attacked by ·OH were the conjugated diene bond, benzene ring, and methoxy group of the Adda side chain.

Based on the molecular weight of the products and the reaction mechanism between ·OH and peptides or protein, three main degradation pathways were proposed as follows: 1) ·OH attacked the conjugated diene bond of Adda side chain through electrophilic addition reaction and produced dihydroxylated-MCLR, and then the hydroxylated C4-C5 or C6-C7 bond of Adda was cleaved through further oxidation to form aldehyde or ketone peptide residues, which were subsequently oxidized into their corresponding carboxylic acids. 2) ·OH attacked the benzene ring and formed benzene hydroxylation and/or benzene dihydroxylation through electrophilic substitution reaction followed by further oxidation to form aldehyde or ketone peptide residues. 3) ·OH attacked the methoxy group of the Adda side chain through hydrogen abstraction reaction to form formic acid-(MCLR), leading to the complete removal of the methoxy group. Pathways 1 and 2 probably accounted for over 90% of the total degradation reactions.

Supporting Information

S1 Fig. The UV254 exposure apparatus for MCLR degradation by UV/H2O2 treatment.
(DOC)

Acknowledgments

This work was supported by a grant from the Key Laboratory Open Fund of Fishery Ecology Environment, Ministry of Agriculture, China.

Author Contributions

Conceived and designed the experiments: ZQF JR YFL. Performed the experiments: YFL JR. Analyzed the data: YFL JR. Contributed reagents/materials/analysis tools: XRW YFL JR FZQ. Wrote the paper: YFL JR.

References

1. Antoniou MG, de-la-Cruz AA and Dionysiou DD, Cyanotoxins: New generation of water contaminants. J Environ Eng-Asce 131: 1239–1243 (2005).
2. Rafael OR and Claudia W, Age related acute effects of microcystin-LR on Daphnia magna biotransformation and oxidative stress. Toxicon 56: 1342–1349 (2010). doi: 10.1016/j.toxicon.2010.07.020 PMID: 20692276
3. Yoshizawa S, Matsushima R, Watanabe MF, Harada K, Ichihara A, Carmichael WW and Fujiki H, Inhibition of protein phosphatases by microcystins and nodularin associated with hepatotoxicity. J Cancer Res Clin 116: 609–614 (1990).
4. Ueno Y, Nagata S, Tsutsumi T, Hasegawa A, Watanabe MF, Park HD, Chen GC, Chen G and Yu SZ, Detection of microcystins, a blue-green algal hepatotoxin, in drinking water sampled in Haimen and Fusui, endemic areas of primary liver cancer in China, by highly sensitive immunoassay. Carcino-genesis 17: 1317–1321 (1996).
5. Carmichael WW, Toxins of cyanobacteria. Sci Am 270: 78–86 (1994). PMID: 8284661
6. Keijola AM, Himberg K, Esala AL, Sivonen K and Hiisvirta L, Removal of cyanobacterial toxins in water treatment processes: laboratory and pilot-scale experiment. Toxicol Assess 81: 102–105 (1988).

7. Falconer IR, Runnergar MTC, Buckley T, Huyn VL and Bradshaw P, Using activated carbon to remove toxicity from drinking water containing cyanobacterial blooms. J Am Water Works Assoc 81: 102–105 (1989).
8. Lee J and Walker HW, Effect of process variables and natural organic matter on removal of microcystin-LR by PAC-UF. Environ Sci Technol 40: 7336–7342 (2006). PMID: 17180986
9. Gao NY, Deng Y and Zhao DD, Ametryn degradation in the ultraviolet (UV) irradiation/hydrogen peroxide (H2O2) treatment. J Hazard Mater 164: 640–645 (2009). doi: 10.1016/j.jhazmat.2008.08.038 PMID: 18824296
10. Liu I, Lawton LA, Cornish B and Rorbertson PKJ, Mechanistic and toxicity studies of the photocatalytic oxidation of microcystin-LR. J Photoch Photobio A 148: 349–354 (2002).
11. Feitz AJ and Waite DT, Kinetic modeling of TiO2-catalyzed photodegradation of trace levels of microcystin-LR. Environ Sci Technol 37: 561–568 (2003). PMID: 12630473
12. Lawton LA, Robertson PKJ, Cornish BJPA and Jaspars M, Detoxification of microcysins (cyanobacterial hepatotoxins) using TiO2 photocatalytic oxidation. Environ Sci Technol 33: 771–775 (1999).
13. Gajdek P, Lechowski Z, Bochnia T and Kepczynski M, Decomposition of microcystin-LR by Fenton oxidation. Toxicon 39: 1575–1578 (2001). PMID: 11478965
14. Bandala ER, Martinez D, Martinez E and Dionysiou DD, Degradation of microcystin-LR toxin by Fenton and photo-Fenton processes. Toxicon 43: 829–832 (2004). PMID: 15284017
15. Song WH, Teshiba T, Rein K and O'Shea KE, Ultrasonically induced degradation and detoxification of microcystin-LR (cyanobacterial toxin). Environ Sci Technol 39: 6300–6305 (2005). PMID: 16173596
16. Song WH, Delacruz AA, Rein K and O'Shea KE, Ultrasonically induced degradation of microcysint-LR and -RR: identification of products, effect of pH, formation and destruction of peroxides. Environ Sci Technol 40: 3941–3946 (2006). PMID: 16830565
17. Antoniou MG, Shoemaker JA, Delacruz AA and Dionysiou DD, Unveiling new degradation intermediates/pathways from the photocatalytic degradation of microcystin-LR and LC/MS/MS structure elucidation of reaction intermediates formed during the TiO2 photocatalysis of microcystin-LR. Environ Sci Technol 42: 8877–8883 (2008). PMID: 19192812
18. Linda IL, Lawton LA and Robertson PKJ, Mechanistic studies of the photocatalytic oxidation of microcystin-LR: an investigation of byproducts of the decomposition process. Environ Sci Technol 37: 3214–3219 (2003). PMID: 12901672
19. Qiao RP, Li N, Qi XH, Wang QS and Zhuang YY, Degradation of microcystin-RR by UV radiation in the presence of hydrogen peroxide. Toxicon 45: 745–752 (2005). PMID: 15804523
20. Lei L, Gao NY, Deng Y, Yao JJ, Zhang KJ, Li HJ, Yin DD, Ou HS and Guo JW, Experimental and model comparisions of H2O2 assisted UV photodegradation of microcystin-LR in simulated drinking water. Journal of Zhejiang Unibersity Science A 11: 1666–1669 (2009).
21. Rosenfeldt EJ and Linden KG, Degradation of endocrine disrupting chemical bisphenol A, ethinyl estradiol, and estradiol during UV photolysis and advanced oxidation processes. Environ Sci Technol 38: 5476–5483 (2004). PMID: 15543754
22. Vogna D, Marotta R, Andreozzi R, Napolitano A and D'Ischia M, Kinetic and chemical assessment of the UV/H2O2 treatment of antiepileptic drug carbamazepine. Chemosphere 54: 497–505 (2004). PMID: 14581052
23. Wu CL, Shemer H and Linden KG, Photodegradation of metolachlor applying UV and UV/H2O2. J Agr Food Chem 55: 4059–4065 (2007).
24. Wu CL and Linden KG, Degradation and byproduct formation of parathion in aqueous solutions by UV and UV/H2O2 treatment. Water Res 42: 4780–4790 (2008). doi: 10.1016/j.watres.2008.08.023 PMID: 18834610
25. Schwarzenbach RP, Gschwend P and Imboden DM, Environmental organic chemistry. Wiley-Interscience, John Wiley and Sons, New York, pp 134 (1993).
26. Onstad GD, Strauch S, Meriluoto J, Codd GA and Von-Gunten U, Selective oxidation of key functional groups in cyanotoxins during drinking water ozonation. Environ Sci Technol 41: 4397–4404 (2007). PMID: 17626442
27. Song WH, Xu T, Cooper WJ, Dionysiou DD, Delacruz AA and O'Shea KE, Radiolysis studies on the destruction of microcystin-LR in aqueous solution by hydroxyl radicals. Environ Sci Technol 43: 1487–1492 (2009). PMID: 19350924
28. Tsuji K, Watanuki T, Kondo F, Watanabe M, Suzuki S, Nakazawa H, Suzuki M, Uchida H and Harada KI, Stability of microcystins from cyanobacterial—II.effect of UV light on decomposition and isomerization. Toxicon 33: 1619–1631 (1995). PMID: 8866619

29. Kaya K and Sano T, A photodetoxification mechanism of the cyanobacterial hepatotoxin microcystin-LR by ultraviolet irradiation. Toxicol 11: 159–163 (1998).

30. McMurry J, Organic Chemistry, 4th Ed, Brooks/Cole Publishing Company: California, pp. 1243 (1995).

31. Buxton GV, Greenstock CL, Helman WP and Ross AB, Critical review of rate constants for reactions of hydrated electrons, hydrogen atoms and hydroxyl radicals (·OH/·O-) in aqueous solution. J Phys Chem Ref 17: 513–886 (1988).

32. Antoniou MG, Shoemaker JA, de-la-Cruz AA and Dionysiou DD, LC/MS/MS structure elucidation of reaction intermediates formed during the TiO2 photocatalysis of microcystin-LR. Toxicon 51: 1103–1118 (2008). doi: 10.1016/j.toxicon.2008.01.018 PMID: 18377943

33. An JS and Carmichael WW, Use of a colorimetric protein-phosphatase inhibition assay and enzyme-linked-immunosorbent-assay for the study of microcystins and nodularins. Toxicon 32: 1495–1507 (1994). PMID: 7725318

34. Barford D and Keller JC, Cocrystallization of the catalytic subunit of the serine threonine specific protein phosphatase-1 from human in complex with microcystin-LR. J Molecular Biol 235: 763–766 (1994).

35. Rinehart KL, Namikoshi M and Choi BW, Structure and biosynthesis of toxins from blue-green-algae (cyanobacteria). J Appl Phycol 6: 159–176 (1994).